Available online at www.sciencedirect.com
SCIENCE DIRECT®
Carbohydrate Research 340 (2005) 181–189
Carbohydrate RESEARCH

Synthesis and NMR characterization of hydroxyurea and mesylglycol glycoconjugates as drug candidates for targeted cancer chemotherapy

Bernd L. Sorg,[a] William E. Hull,[b] Hans-Christian Kliem,[a] Walter Mier[c] and Manfred Wiessler[a,*]

[a]*Division of Molecular Toxicology, German Cancer Research Center (DKFZ), Im Neuenheimer Feld 280, D-69120 Heidelberg, Germany*
[b]*Central Spectroscopy Department, German Cancer Research Center (DKFZ), Im Neuenheimer Feld 280, D-69120 Heidelberg, Germany*
[c]*Division of Nuclear Medicine, University Hospital Heidelberg, Im Neuenheimer Feld 400, D-69120 Heidelberg, Germany*

Received 4 April 2004; accepted 26 November 2004

Abstract—Tumor targeting of glycoconjugated antineoplastic agents is a strategy currently under investigation for cancer chemotherapy. We have synthesized the glucosides and galactosides of the clinically established drug hydroxyurea and of mesylglycol, the reactive moiety of the anticancer drug busulfan. Glycosides of hydroxyurea were obtained by carbamoylation of hydroxylamine glycosides. The glycosides of mesylglycol were synthesized by mesylation of protected glycol glycosides. All compounds were characterized by detailed ^{1}H and ^{13}C NMR analysis.

Keywords: Anticancer drugs; Targeting; Glucose transport proteins; ADEPT; Hydroxyurea; Mesylglycol

1. Introduction

In cancer chemotherapy the practical clinical use of classical antineoplastic drugs is generally limited by dose-dependent toxic side effects, primarily caused by the nonspecific distribution of common drugs in the body following systemic administration.[1,2] Consequently, protocols with sub-optimal doses of drugs are frequently used, minimizing toxicity and patient suffering but possibly resulting in incomplete therapy with unsatisfactory prognosis (residual disease, tumor regrowth, drug resistance).

Therefore, to improve the specificity of cancer therapy, drugs with tumor-targeting properties are under development and in clinical trials. These drugs are designed to achieve high concentrations selectively in the target tissue.[1,2] Such agents can often be described as *prodrugs* since the actual toxic agent is then generated or released in situ, while minimizing the systemic load of toxic metabolites. In this respect, there are two main mechanisms whereby monoglycosylated anticancer drugs can prove to be advantageous: (1) strongly increased consumption of monosaccharides by tumor compared to normal cells[3–5] may lead to enhanced intracellular uptake of glycosylated drugs in tumor cells, possibly mediated by glucose transport proteins; (2) the activation or release of the glycoconjugated drug at the target site can be expedited by glycosidases linked to tumor-specific antibodies.[2,6]

1-*O*-Glucosides and galactosides can be transported by sodium-coupled glucose transport (SGLT) proteins.[7,8] Recent investigations have shown that glucosides of 2-naphthol or hydroxyindole are accepted as substrates by SGLTs; this gives an indication of the possible size of the glucose-linked moiety.[8] The first anticancer agent designed to exploit mechanism (1) is the new drug glufosfamide, the glucoside of the antineoplastic agent ifosfamide mustard.[9] It has been shown in animal experiments that glufosfamide accumulates in tumor tissue.[10] Furthermore, it has been shown in

* Corresponding author. Tel.: +49 6221 423311; fax: +49 6221 423375; e-mail: m.wiessler@dkfz.de

0008-6215/$ - see front matter © 2004 Published by Elsevier Ltd.
doi:10.1016/j.carres.2004.11.024

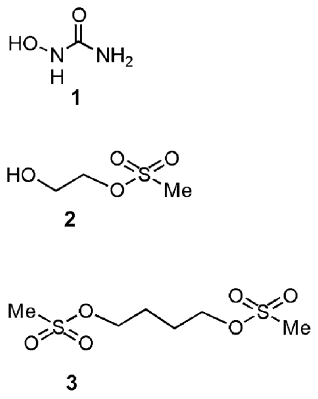

Figure 1. Structures of hydroxyurea (**1**), mesylglycol (**2**), and busulfan (**3**).

electrophysiological studies that glufosfamide can be actively transported into cells by the porcine glucose transport protein SGLT3.[11] However, data demonstrating transport by analogous human transport proteins have not yet been published. Glufosfamide has been successfully tested in a phase II clinical trial.[12]

The second mechanism of tumor targeting with prodrugs based on glucosides or galactosides of anticancer therapeutics involves the activation of the conjugated drug via antibody-linked glycosidases, which are directed against tumor cells, a concept generally known as antibody-directed enzyme prodrug therapy (ADEPT).[6] ADEPT strategies commonly use galactosidase, carboxypeptidase, or nitroreductase,[2] and ADEPT systems are currently in phase I clinical trials.[13] Selective cytotoxicity of drug-linked glucosides and galactosides has been shown in cell culture studies.[14,15]

Therefore, we describe the synthesis and characterization of the glucosides and galactosides of the anticancer drug hydroxyurea (**1**, Fig. 1), a clinically established inhibitor of DNA synthesis,[16,17] and of the DNA-alkylating compound mesylglycol (**2**),[18] a derivative of the therapeutically used anticancer drug busulfan (**3**).[19] Hydroxyurea (**1**) and mesylglycol (**2**) represent two of the smallest molecules known to possess cytostatic activity, and their glycoconjugates may meet the requirements for transporter-mediated drug targeting. Furthermore, the synthesized glycoconjugates are drug candidates for ADEPT.

2. Results and discussion

2.1. Synthesis of the glycosides of hydroxyurea (ureido glycosides 11, 12; Scheme 1)

Due to its high polarity, hydroxyurea (**1**) is quite insoluble in the organic solvents generally used in glycosylation reactions (e.g., dichloromethane, diethyl ether, acetonitrile). Thus, the typical conditions for standard procedures such as the trichloroacetimidate method[20,22] or the Koenigs–Knorr method[21,22] could not be applied for the direct glycosylation of hydroxyurea (**1**). Therefore, the synthesis was attempted with benzyl-protected glucose α-D-trichloroacetimidate as glycosyl donor in either ethyl acetate or acetonitrile at +50 °C, as for the synthesis of glufosfamide.[11] However, this strategy was not successful in preparing ureido glycosides. Furthermore, phase-transfer-catalyzed glycosylation of hydroxyurea (**1**) with acetylated glycosyl bromides under the conditions described for conjugation of *N*-hydroxysuccinimide (**6**)[23] led to no product and only partially deacetylated and debrominated glucose species were detected.

Thus, in our subsequent work we did not attempt the direct glycosylation of hydroxyurea but rather the generation of ureido glycosides by the addition of cyanate to hydroxylamino glycosides. To this end, the protected glucoside **7** and galactoside **8** were synthesized by phase-transfer-catalyzed glycosylation of *N*-hydroxysuccinimide (**6**) with tetra-*O*-acetyl-α-D-glucopyranosyl bromide (**4**) and tetra-*O*-acetyl-α-D-galactopyranosyl bromide (**5**) as described by Cao et al.[23] for the galactoside **8**. The subsequent deprotection of the glycosides **7** and **8** to their corresponding hydroxylamine derivatives **9** and **10** was achieved using 5 M methanolic NH_4OH at +75 °C (C. Bertozzi, *personal communication*) instead of ethanolic hydrazine at room temperature.[23] This method considerably simplified the purification of the products, which could be isolated by column chromatography. Coupling of the hydroxylamine glycosides **9** and **10** with cyanate was performed in an aqueous solution with equimolar amounts of HCl present. The target glycosides, ureido glucoside (**11**) and ureido galactoside (**12**), were obtained in high yields (**11**: 75%; **12**: 85%). Purification of the compounds for use in biological experiments was done by preparative HPLC.

2.2. Synthesis of the glycosides of mesylglycol (19 and 20; Scheme 2)

Although Helferich and Werner synthesized the acetyl-protected glucoside of mesylglycol **17** as a precursor to 1,6-ethylene-linked glucose in 1942,[24] the title compounds **19** and **20** have not yet been described in the literature. According to the method of Helferich and Werner,[24] acetyl-protected glycosides of ethylene glycol (**14**, **15**) were reacted with mesylchloride (**16**) in pyridine to give the protected glycosides of mesylglycol (**17**, **18**). The glucoside **17** crystallized spontaneously from the reaction mixture, whereas the galactoside **18** was obtained as a colorless syrup after column chromatography. Deprotection of both compounds was achieved by the Zemplén procedure[25] using NaOMe in MeOH at room temperature and resulted in the title compounds **19** and **20**, which were purified by recrystallization from ethyl acetate.

2.3. Characterization of the glycosides by NMR

Detailed NMR signal assignments, chemical shifts, and *J* couplings are summarized for several of the synthesized glycosides in Tables 1–3. Most of the ^{1}H spectra are highly complex, with strong signal overlap and second-order effects evident even at 500 MHz, and, therefore, required spin system simulation for complete analysis (see Section 3). The comprehensive data obtained not only confirm the β-glycoside structures with $^4C_1$ ring conformation, as presented in Schemes 1 and 2, but also provide a number of useful insights into the structure dependence of the NMR parameters.

In DMSO-d_6 all hydroxyl protons are well-resolved with the following ordering of chemical shifts: glucosides (2-OH > 3 > 4 > 6); galactosides (2-OH > 3 > 6 > 4), with an axial 4-OH shifted ca. 0.5 ppm upfield relative to an equatorial 4-OH (**12** vs **11**). The $^3J_{HOCH}$ couplings of the hydroxyls range between 4.5 and 6.7 Hz and are generally different for each ring position and also for H-6a versus H-6b and H-8a versus H-8b in the ethyleneglycol derivatives, indicating nonequal hydroxyl rotamer populations.

Ring proton chemical shifts for unprotected derivatives are H-1 > 6b > 6a > 3 > 5 > 4 > 2 for glucosides **9**, **11**, **19** and H-1 > 4 > 6b > 6a > 5 > 2 > 3 for galactosides **12** and **20**. For peracetylated compounds the shift order is H-3 > 4 > 2 > 1 > 6b > 6a > 5 for glucosides **14** and **17** and H-4 > 2 > 3 > 1 > 6b > 6a > 5 for galactosides **15** and **18**. The specific assignments obtained for the acetyl methyl groups indicate that the chemical shift patterns are 6-Ac > 2 > 4 > 3 for glucosides and 4-Ac > 2 > 6 > 3 for galactosides.

For glucosides **9**, **11**, **19** the stereochemical assignments H-6b = H-6(*Si*) and H-6a = H-6′(*Re*) can be made based on the small $J_{5,6b}$ coupling (*gg* and *gt* conformers predominate, H-6b is 0.2 ppm *downfield* of H-6a). For the peracetylated glucosides **14** and **17**, H-6(*Si*) can be assigned to the *upfield* proton H-6a. For the galactosides the nearly equal chemical shifts for H-6a and H-6b and large (>5 Hz) couplings to H-5 indicate a predominance of *gt* and *tg* conformers. The ethyl fragments in the glycol substituents exhibit the complex multiplets associated with nonequal rotamer populations, and the magnitudes of the coupling constants are consistent with the predominance of the *trans* orientation of O-1 and O-8 and unequal populations of the two possible *gauche* rotamers.

The ^{13}C NMR data show the expected trends for galactose versus glucose while the chemical shift order C-7 > C-8 for the ethyleneglycol substituent is reversed to C-8 > C-7 in mesylglycol. The specific assignments

Table 1. ^{1}H NMR chemical shifts (in ppm) for the glycosides **9**, **11**, **12**, **14**, **15**, **17**–**20**[a]

Compound	**9**	**11**	**19**	**14**	**17**	**12**	**20**	**15**	**18**
Solvent	DMSO-d_6	DMSO-d_6	CD_3OD	$CDCl_3$	$CDCl_3$	DMSO-d_6	CD_3OD	$CDCl_3$	$CDCl_3$
Temp.	37 °C	37 °C	30 °C	30 °C	30, 27 °C	40 °C	30, 27 °C	30, 27 °C	30 °C
^{1}H Freq.	250	500	250	250	500, 300	500	500, 300	250, 300	250
Sugar	Glc	Glc	Glc	Glc	Glc	Gal	Gal	Gal	Gal
R	OH	OH	OD	OAc	OAc	OH	OD	OAc	OAc
β1-O–R′	$–NH_2$	$–NHC(O)NH_2$	$–EtOSO_2Me$	–EtOH	$–EtOSO_2Me$	$–NHC(O)NH_2$	$–EtOSO_2Me$	–EtOH	$–EtOSO_2Me$
Pos.[b] 1	4.230	4.333	4.335	4.558	4.577	4.295	4.293	4.534	4.539
2	2.975	3.044	3.204	5.012	5.003	3.368	3.532	5.215	5.209
3	3.129	3.188	3.360	5.222	5.215	3.335	3.480	5.041	5.030
4	3.004	3.059	3.288	5.062	5.083	3.641	3.835	5.398	5.402
5	3.085	3.162	3.290	*3.72–3.75*	3.724	3.404	3.533	3.972	3.932
6a	3.423	3.453	3.670	4.190	4.159	3.495	3.726	4.157	4.135
6b	3.661	3.675	3.874	4.203	4.259	3.544	3.768	4.159	4.179
7a	6.152	9.201	3.886	3.841	3.845	9.180	3.889	3.833	3.845
7b			4.117	3.846	4.078		4.116	3.866	4.098
8a			4.414	*3.698*	4.347		4.416	3.713	4.356
8b			4.433	*3.761*	4.365		4.434	3.737	4.368
9		6.525	3.123	2.423	3.032	6.510	3.128	2.609	3.038
2-R	4.923	5.584		2.057	2.063	5.417		2.072	2.079
3-R	4.831	4.996		2.009	2.006	4.714		1.988	1.988
4-R	4.799	4.895		2.032	2.029	4.369		2.162	2.158
6-R	4.402	4.399		2.095	2.093	4.471		2.063	2.057

[a] NMR measurements were performed using the solvents, temperatures, and proton frequencies given; chemical shifts are in ppm relative to the references specified in Section 3. The sugar moiety (Glc or Gal), the sugar ring substituents R at C-2, C-3, C-4, C-6, and the substituent R′ at C-1β are listed. All data presented are the result of spin system simulations using WinDaisy (see Section 3). Values in italics for **14** represent approximate values where an unequivocal simulation solution could not be achieved.

[b] The conventional numbering scheme for hexoses is used; a and b refer to low-frequency and high-frequency resonances; pos. 7, 8, 9 refer to the C-1-O-substituent R′: pos. 7 = $–NH_2$ in **9**, –NH– in **11**, **12**, and $–OCH_2–$ in the glycol derivatives; pos. 8 = C=O in ureido derivatives and $–CH_2O–$ in the glycol derivatives; pos. 9 = $–NH_2$ in ureido derivatives, –OH in ethyleneglycol and $–OSO_2Me$ in mesylglycol.

Table 2. ^{1}H NMR coupling constants (in Hz) for the glycosides of Table 1[a]

Compound	**9**	**11**	**19**	**14**	**17**	**12**	**20**	**15**	**18**
Solvent	DMSO-d_6	DMSO-d_6	CD_3OD	$CDCl_3$	$CDCl_3$	DMSO-d_6	CD_3OD	$CDCl_3$	$CDCl_3$
Temp.	37 °C	37 °C	30 °C	30 °C	30, 27 °C	40 °C	30, 27 °C	30, 27 °C	30 °C
^{1}H Freq.	250	500	250	250	500, 300	500	500, 300	250, 300	250
Sugar	Glc	Glc	Glc	Glc	Glc	Gal	Gal	Gal	Gal
R	OH	OH	OD	OAc	OAc	OH	OD	OAc	OAc
β1-O–R′	$-NH_2$	$-NHC(O)NH_2$	$-EtOSO_2Me$	–EtOH	$-EtOSO_2Me$	$-NHC(O)NH_2$	$-EtOSO_2Me$	–EtOH	$-EtOSO_2Me$
Pos.[b] 1,2	8.16	8.25	7.82	8.00	7.96	8.18	7.75	7.99	7.98
2,3	9.20	9.05	9.30	9.80	9.65	9.40	9.69	10.48	10.49
3,4	8.60	8.89	8.90	9.50	9.42	3.35	3.47	3.47	3.45
4,5	9.60	9.68	9.80	10.10	10.08	1.11	1.14	1.16	1.22
5,6a	6.50	6.03	5.73	3.60	2.42	6.20	5.19	7.13	6.74
5,6b	2.60	2.22	2.06	4.20	4.84	6.12	6.98	6.07	6.50
6a,6b	−11.70	−11.69	−11.91	−12.20	−12.36	−10.81	−11.36	−11.90*	−11.16
7a,7b			−12.15	*−11.3**	−11.79		−12.14	−11.18	−11.74
7a,8a,			2.90	*6.65*	7.32		2.90	6.12	7.49
7a,8b			6.62	*2.10*	3.01		6.70	2.75	2.89
7b,8a			5.88	*1.87*	2.98		5.88	2.60	2.78
7b,8b			2.92	*6.86*	5.23		2.86	6.45	5.11
8a,8b			−11.45	*−12.6**	−11.63		−11.47	−12.57	−11.61
2,2-OH	4.85	4.57				4.54			
3,3-OH	4.58	4.90				5.82			
4,4-OH	4.85	5.45				4.73			
6a,6-OH	6.70	5.43				4.92			
6b,6-OH	5.37	6.17				6.50			
8a,8-OH				7.06				7.02	
8b,8-OH				5.92				5.77	
^4J 1,3						−0.20	−0.18		
2,4						−0.51	−0.42		
5,4-OH						0.60			

[a] See footnote to Table 1; all data are the result of iterative WinDaisy simulations with the following exceptions: for **9** a simple lineshape deconvolution analysis of –OH groups was performed with WINNMR; the ring protons for **9** were analyzed by manual iteration for a spectrum obtained after exchanging –OH to –OD with D_2O, and the reported chemical shifts were corrected for the deuterium isotope effect observed at H-1 (−0.0056 ppm); values in italics for **14** are preliminary due to strong overlap; values marked with * were set manually and kept fixed during iteration. The negative signs for ^4J couplings in Gal were confirmed by simulations at 300 and 500 MHz.

[b] Coupling partners are given using the numbering scheme of Table 1.

for the acetyl groups reveal that the carbonyl carbon shifts follow the order 6-Ac > 3 > 2 > 4 in the glucosides and 6-Ac > 4 > 3 > 2 in the galactosides.

3. Experimental

3.1. General methods

All solvents and reagents were reagent grade and were used without further purification. Solutions were evaporated under reduced pressure at a bath temperature below 40 °C. Thin-layer chromatography (TLC) was performed on silica gel plates (Polygram Sil G/UV_{254}, Macherey & Nagel, Germany), and detection was achieved by spraying with 0.1% vanillin in 50% H_2SO_4 (aq) followed by heating. Column chromatography was done on silica gel (Kieselgel 60, 70–230 mesh or 230–400 mesh, Macherey & Nagel, Germany). Uncorrected melting points were determined on a Büchi SMP 20 melting-point apparatus. Optical rotation was measured with a Perkin–Elmer 241 polarimeter at 20 °C with a path length of 0.1 m; the concentration for the optical rotation $[\alpha]_D^{20}$ is given in g/100 mL. Mass spectrometry (ESI-MS, *m*/*z* precision ± 0.1) was performed on a Finnigan MAT TSQ 7000. High-resolution mass spectra (FAB-MS, *m*/*z* precision ±0.0001) were obtained with a JEOL JMS-SX 102A mass spectrometer. Elemental analyses were obtained with a Carlo Erba CHNS EA 1108 Elemental Analyzer. For two compounds (**11**, **12**), which could not be completely dried, appropriate numbers of water molecules were added to the chemical formula to give the best fit to the elemental analysis data.

3.2. NMR analysis

NMR spectra for various compounds were recorded at 250, 300, or 500 MHz (^{1}H) and at 62.9, 75.5, or 125.8 MHz (^{13}C) on Bruker AC-250, AM-300, or AM-500 spectrometers, respectively, using 5 mm sample tubes and conventional pulsed Fourier NMR

Table 3. ^{13}C NMR chemical shifts (in ppm) for the compounds of Table 1[a]

Compound	**9**	**11**	**19**	**14**	**17**	**12**	**20**	**15**	**18**
Solvent	DMSO-d_6	DMSO-d_6	CD_3OD	$CDCl_3$	$CDCl_3$	DMSO-d_6	CD_3OD	$CDCl_3$	$CDCl_3$
Temp.	37 °C	37 °C	30 °C	30 °C	30, 27 °C	40 °C	30, 27 °C	30, 27 °C	30 °C
^1H Freq.	250	500	250	250	500, 300	500	500, 300	250, 300	250
Sugar	Glc	Glc	Glc	Glc	Glc	Gal	Gal	Gal	Gal
R	OH	OH	OD	OAc	OAc	OH	OD	OAc	OAc
β1-O–R′	$–NH_2$	$–NHC(O)NH_2$	$–EtOSO_2Me$	–EtOH	$–EtOSO_2Me$	$–NHC(O)NH_2$	$–EtOSO_2Me$	–EtOH	$–EtOSO_2Me$
Pos. 1	106.06	106.95	104.53	101.47	100.84	107.61	105.10	101.82	101.33
2	71.98	71.79	75.03	71.39	71.04	69.11	72.44	68.87	68.55
3	76.57	76.36	*78.04*	72.70	72.59	73.21	74.92	70.74	70.72
4	70.15	69.78	71.58	68.49	68.28	67.87	70.31	66.99	66.97
5	76.80	76.90	*78.06*	71.98	72.02	75.34	76.79	70.84	70.95
6	61.25	60.99	62.75	*62.01*	61.79	60.19	62.56	61.49	61.25
7			68.53	73.15	67.37		68.43	72.88	67.27
8		161.08	71.01	*62.08*	68.62	161.21	71.06	61.82	68.65
S–Me			37.59		37.52		37.59		37.48
2-Ac (C=O)				169.45	169.44			169.57	169.60
(Me)				20.67	20.64			20.69	20.73
3-Ac (C=O)				170.20	170.16			170.01	170.05
(Me)				20.58	20.57			20.46	20.53
4-Ac (C=O)				169.40	169.40			170.12	170.13
(Me)				20.58	20.57			20.55	20.64
6-Ac (C=O)				170.60	170.60			170.34	170.37
(Me)				20.68	20.71			20.53	20.62

[a] See footnote to Table 1. Assignments are based on CH correlations obtained for compounds **11**, **12**, **15**, **17**, **20**. The few remaining uncertainties are noted in italics.

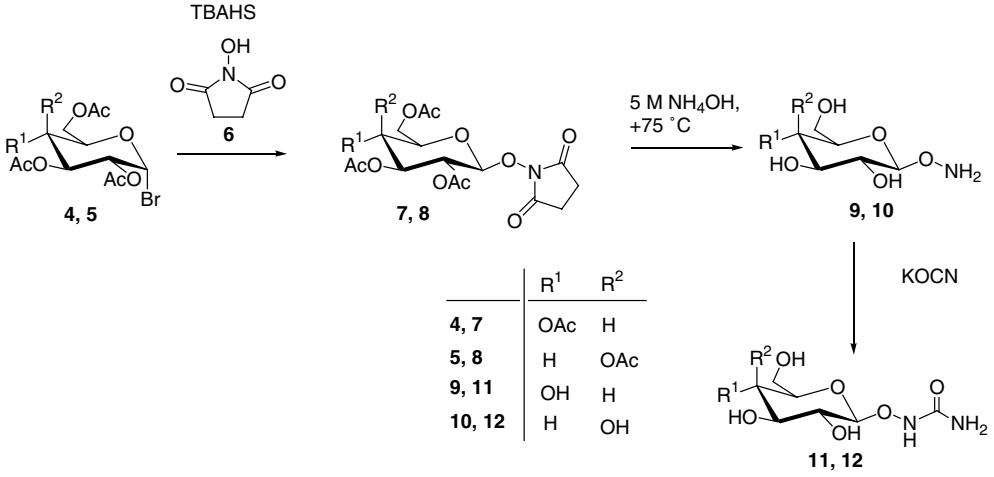

Scheme 1. Synthesis of glycosides of hydroxyurea (TBAHS = *tert*-butyl-ammonium hydrogen sulfate).

techniques. Depending on solvent, the following $^1H/^{13}C$ chemical shift references (in ppm) were used: in $CDCl_3$, tetramethyl silane (TMS) = 0.0, $^{13}CDCl_3$ = 77.03; in DMSO-d_6, DMSO-d_5 = 2.490, DMSO-d_6 = 39.50; in CD_3OD, CHD_2OD = 3.310, $^{13}CD_3OD$ = 49.053. The one-dimensional ^1H spectra were analyzed with Lorentz–Gauss resolution enhancement, initially as first-order multiplet analysis with the Bruker WINNMR software for PCs and then with separate spectrum simulations for the sugar and glycol fragments using Bruker's WinDaisy spin system analysis software (Tables 1 and 2). For each compound strong second-order effects were observed for at least some portion of the spin systems involved. When present, sugar hydroxyl protons were included in the analysis. Whenever possible, the WinDaisy analysis was executed with full least-squares iterative lineshape fitting (max. 10 spins) to determine chemical shifts, couplings, and linewidths with standard deviations of generally $\leqslant$0.03 Hz and frequently <0.01 Hz. In some cases manual or mixed manual/iterative adjustment of ring proton parameters was necessary (**9**, **14**, **19**).

The glucose and galactose ^1H spin systems for C-1–C-6 were directly assignable from the analysis of coupling constants, with exception of the acetyl methyl groups in protected sugars. The two pairs of methylene protons at

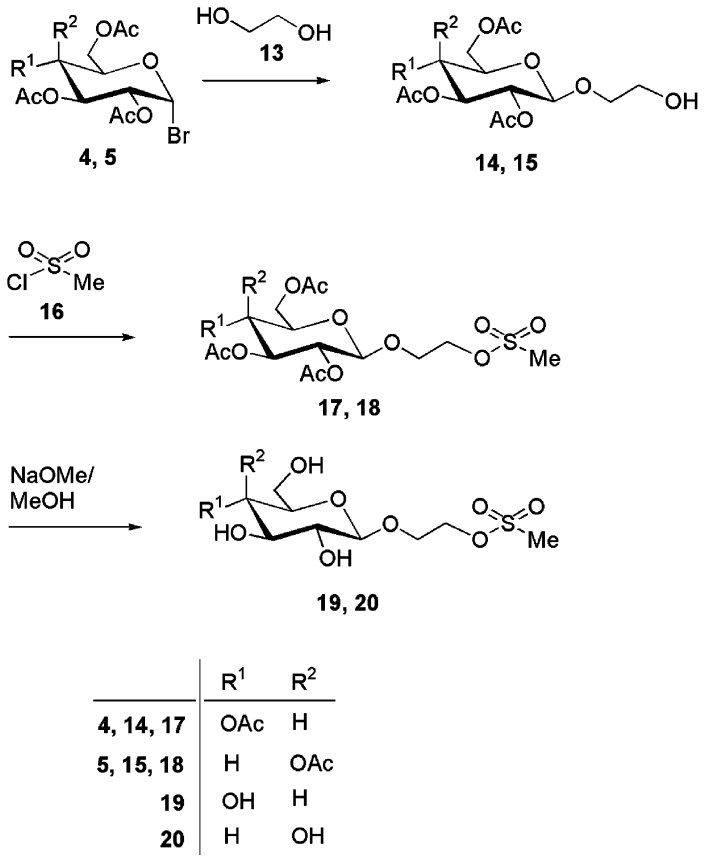

	R^1	R^2
4, 14, 17	OAc	H
5, 15, 18	H	OAc
19	OH	H
20	H	OH

Scheme 2. Synthesis of glycosides of mesylglycol.

C-7 and C-8 in the ethyleneglycol (–O–C^7H_2–C^8H_2–OH) and mesylglycol substituents (–O–C^7H_2–C^8H_2–OSO_2Me) were nonequivalent in all cases. The ethyleneglycol protons H-8a,b could be readily distinguished from the H-7a,b protons (at higher frequencies) on the basis of their couplings to the terminal –OH group. This discrimination was not possible for the mesylglycol group; therefore, nuclear Overhauser (NOE) difference spectra were acquired for compound **17** at 500 MHz with the following results (% NOE): saturation at H-1 gave NOEs at H-2 (2.2), H-3 (5.6), H-5 (11.7), H-7a (5.6), H-7b (2.9), H-8a,b (3.4); saturation of the S–Me group gave a measurable NOE only at H-8a,b (0.81). These results confirmed that in the mesylglycol group H-7a,b resonate at lower frequencies relative to H-8a,b and exhibit a larger shift difference due to the influence of the asymmetric center C-1. Complete and unequivocal WinDaisy analyses were obtained for all compounds except for the ethyleneglycol group of **14**, where H-8a,b overlapped completely with H-5; in this case the results must be viewed as preliminary estimates. The WinDaisy analysis also revealed ^4J couplings (H-1,3; H-2,4; H-5,4-OH; see Table 2) in the galactose spin system for compounds **12** and **20**, which were measured with the highest possible resolution at 500 MHz. Finally, two-dimensional H,H-COSY experiments were used only for unprotected glycosides in DMSO-d_6 solution in order to confirm hydroxyl proton assignments.

One-dimensional ^{13}C NMR spectra, broadband ^1H-decoupled and DEPT (135°), were recorded for all compounds (Table 3). In several cases two-dimensional experiments for ^1J CH correlation (BIRD-PT-R with decoupling of remote protons[26,27]) and long-range CH correlation (COLOC-S[27,28] optimized for $^nJ = 6$ Hz) were performed to provide unequivocal carbon resonance assignments for compounds **11**, **12**, **15**, **17**, **20** via the ^1H assignments. The long-range correlation experiments provided connectivities between H-1 and C-7 of the ethyleneglycol or mesylglycol substituent as well as the necessary connectivities to assign the methyl and carbonyl signals of the acetyl groups. The assignments obtained with 2D methods were readily transferred by analogy to compounds **9**, **14**, **18**, **19**. The few remaining uncertainties are noted in Table 3.

3.3. Preparative HPLC for the purification of compounds 11–12

Preparative HPLC was performed on a Merck aminophase LiChrospher-100 NH_2 column (5 μm,

250 mm × 25 mm) with a Latek P400 pump system with a Rheodyne injection valve and a Shimazu UV variable-wavelength detector set at 200 nm. The eluent was 80:20 CH_3CN–H_2O at a flow rate of 10 mL/min.

3.4. *O*-(2,3,4,6-Tetra-*O*-acetyl-β-D-glucopyranosyl)-*N*-hydroxysuccinimide (7), *O*-(2,3,4,6-tetra-*O*-acetyl-β-D-galactopyranosyl)-*N*-hydroxysuccinimide (8), and *O*-(β-D-galactopyranosyl)hydroxylamine (10)

Compounds **7**, **8**, and **10** were synthesized according to literature procedures.[23]

3.5. *O*-(β-D-Glucopyranosyl)hydroxylamine (9)

Compound **7** (4.00 g, 9.0 mmol) was suspended in 63 mL of methanol. To this mixture, 37 mL of a 25% aqueous solution of NH_3 was added, and the reaction mixture was heated at 75 °C for 16 h. After evaporation of the solvents the product was purified by column chromatography (silica gel, CH_3CN–H_2O–Et_3N 85:10:5). The organic solvents were removed in vacuo, and the remaining aqueous solution was lyophilized. Compound **9** was obtained as a white foam. Yield: 1.60 g (91%); R_f 0.19 (CH_3CN–H_2O–Et_3N 87.5:7.5:5); ESI-MS: *m*/*z* 390.9 (calcd 391.156 for $[2M+H]^+$, $M = 195.074$ for $C_6H_{13}NO_6$). NMR data for this compound and all others discussed below are summarized for comparison in Tables 1–3.

3.6. *N*-(β-D-Glucopyranosyloxy)urea (11)

Compound **9** (1.36 g, 7.0 mmol) and KOCN (1.13 g, 13.9 mmol) were dissolved in 120 mL H_2O at room temperature. To start the reaction, 1 M HCl (ca. 7 mL) was added slowly until a new product with slightly higher R_f value (R_f 0.20) was observed by TLC (CH_2Cl_2–MeOH 4:1). Purification was achieved using column chromatography (silica gel, CH_3CN–H_2O–Et_3N 85:10:5). The organic solvents were removed in vacuo, and the remaining aqueous solution was lyophilized. Compound **11** was obtained as a white foam. Yield: 1.25 g (75%). Analytical samples were obtained by prep. HPLC (see Section 3.3); R_f 0.20 (CH_3CN–H_2O–Et_3N 85:10:5); $[\alpha]_D^{20}$ −34.8 (*c* 0.94, H_2O); positive-ion FAB-MS: *m*/*z* 239.0882 (calcd 239.0874 for $[M+H]^+$, $M = 238.080$ for $C_7H_{14}N_2O_7$). Anal. Calcd for $5C_7H_{14}N_2O_7 + 2H_2O$: C, 34.26; H, 6.08; N, 11.42. Found: C, 34.31; H, 6.14; N, 11.42.

3.7. *N*-(β-D-Galactopyranosyloxy)urea (12)

Compound **12** was synthesized as described for compound **11** starting from 1.68 g (8.6 mmol) of **10** and 1.40 g (17.3 mmol) KOCN in 160 mL of H_2O with ca. 8 mL 1 M HCl to yield 1.74 g (85%) as a white foam; R_f 0.18 (CH_3CN–H_2O–Et_3N 85:10:5); $[\alpha]_D^{20}$ −5.7 (*c* 1.07, H_2O); positive-ion FAB-MS: *m*/*z* 239.0885 (calcd 239.0874 for $[M+H]^+$, $M = 238.080$ for $C_7H_{14}N_2O_7$). Anal. Calcd for $5C_7H_{14}N_2O_7 + 4H_2O$: C, 33.28; H, 6.22; N, 11.09. Found: C, 33.34; H, 6.26; N, 11.10.

3.8. 1-(2,3,4,6-Tetra-*O*-acetyl-β-D-glucopyranosyloxy)-2-hydroxyethane (14)

In 40 mL dry CH_3CN with ca. 4 g molecular sieve (3 Å), 3.57 g (16.5 mmol) HgO, 0.99 g (2.8 mmol) $HgBr_2$, and 10.28 g (25.0 mmol)[29] tetra-*O*-acetyl-α-D-glucopyranosyl bromide (**4**) were added with stirring. Subsequently, 4.2 mL (4.66 g, 75.1 mmol) freshly distilled ethylene glycol were added, and the reaction mixture was stirred for 16 h at room temperature. The mixture was filtered and evaporated in vacuo. The residue was dissolved in EtOAc (40 mL) and extracted with brine (2 × 20 mL) and H_2O (2 × 20 mL). The organic solvent was dried over Na_2SO_4, filtered and evaporated. The product was purified using column chromatography (silica gel, petroleum ether–EtOAc 3:4). Yield: 4.48 g (46%) of pure β-anomer, 1.81 g (19%) of α/β mixture; R_f β-anomer 0.20 (petroleum ether–EtOAc 3:4); ESI-MS *m*/*z* 414.9 (calcd 415.121 for $[M+Na]^+$, $M = 392.132$ for $C_{16}H_{24}O_{11}$).

3.9. 1-(2,3,4,6-Tetra-*O*-acetyl-β-D-galactopyranosyl-oxy)-2-hydroxyethane (15)

Compound **15** was prepared from **5** as described for compound **14**. Yield: 5.41 g (55%) of pure β-anomer, 0.43 g (4%) of α/β mixture; R_f β-anomer 0.20 (petroleum ether–EtOAc 3:4); ESI-MS *m*/*z* 415.0 (calcd 415.121 for $[M+Na]^+$, $M = 392.132$ for $C_{16}H_{24}O_{11}$). The spectroscopic data agree well with those in the literature.[30]

3.10. 1-(2,3,4,6-Tetra-*O*-acetyl-β-D-glucopyranosyloxy)-2-(methanesulfonyloxy)ethane (17)

Compound **17** was synthesized according to the literature methods[24] with minor modifications. Compound **14** (4.35 g, 11.1 mmol) was dissolved in 4.4 mL of pyridine. The solution was cooled to 0 °C and 1.3 mL mesylchloride (**16**) (1.92 g, 16.8 mmol) were slowly added. The reaction mixture was stirred at room temperature for 6 h. H_2O (2.2 mL) was added to quench the unreacted mesylchloride (**16**). An additional 35 mL H_2O was added, resulting in the separation of a colorless syrup from the reaction mixture. This syrup crystallized spontaneously or after scratching the flask with a glass rod. The crystalline raw product was collected by filtration, and the residue was extracted twice with CH_2Cl_2

(2×40 mL). The organic phase was extracted with brine (2×80 mL), washed with water (2×80 mL), and dried over Na_2SO_4. The solvent was removed under reduced pressure. The raw product was recrystallized from EtOAc to yield the pure compound **17** (3.22 g, 62%; 67% according to Ref. 22) as white needles; mp 90 °C; R_f 0.24 (petroleum ether–EtOAc 1:1); $[\alpha]_D^{20}$ −16.1 (*c* 0.94, H_2O); ESI-MS: *m/z* 493.0 (calcd 493.099 for $[M+Na]^+$, $M = 470.109$ for $C_{17}H_{26}O_{13}S$). Anal. Calcd for $C_{17}H_{26}O_{13}S$: C, 43.40; H, 5.57; S, 6.82. Found: C, 43.21; H, 5.65; S, 6.86.

3.11. 1-(2,3,4,6-Tetra-*O*-acetyl-β-D-galactopyranosyloxy)-2-(methanesulfonyloxy)ethane (18)

Compound **18** was synthesized as described for **17**, using 5.20 g (13.3 mmol) of compound **15**. The purification was achieved using column chromatography (silica gel, petroleum ether–EtOAc 1:1). Yield: 3.58 g (57%). Analytical samples were prepared by recrystallization from EtOAc; R_f 0.22 (petroleum ether–EtOAc 1:1); $[\alpha]_D^{20}$ 0 (*c* 0.72, H_2O); ESI-MS: *m/z* 492.9 (calcd 493.099 for $[M+Na]^+$, $M = 470.109$ for $C_{17}H_{26}O_{13}S$). Anal. Calcd for $C_{17}H_{26}O_{13}S$: C, 43.40; H, 5.57; S, 6.82. Found: C, 43.57; H, 5.68; S, 6.76.

3.12. 1-(β-D-Glucopyranosyloxy)-2-(methanesulfonyloxy)ethane (19)

Compound **17** (3.22 g, 6.8 mmol) was dissolved in 40 mL of MeOH. To this mixture 10 mL of 0.1 M NaOMe in MeOH were added. The solution was stirred for 20 min at room temperature. The reaction mixture was neutralized using the ion-exchange resin Amberlite H^+ 50 WX 2, filtered, and evaporated. Purification was done by column chromatography (silica gel, CH_2Cl_2–MeOH 9:1). Yield: 1.58 g (76%). Analytical samples of **19** were obtained by recrystallization from EtOAc; mp 76 °C; R_f 0.16 (CH_2Cl_2–MeOH 9:1); $[\alpha]_D^{20}$ −25.2 (*c* 0.97, H_2O); ESI-MS: *m/z* 627.0 (calcd 627.124 for $[2M+Na]^+$, $M = 302.067$ for $C_9H_{18}O_9S$). Anal. Calcd for $C_9H_{18}O_9S$: C, 35.76; H, 6.00; S, 10.61. Found: C, 35.94; H, 5.88; S, 10.65.

3.13. 1-(β-D-Galactopyranosyloxy)-2-(methanesulfonyloxy)ethane (20)

Compound **20** was obtained by deprotection of **18** using the procedure described for compound **19**. The crude reaction mixture was purified by recrystallization from EtOAc without prior column chromatography. Yield: 1.92 g (86%); mp 89 °C; R_f 0.16 (CH_2Cl_2–MeOH 9:1); $[\alpha]_D^{20}$ 0 (*c* 1.32, H_2O); ESI-MS: *m/z* 627.0 (calcd 627.124 for $[2M+Na]^+$, $M = 302.067$ for $C_9H_{18}O_9S$). Anal. Calcd for $C_9H_{18}O_9S$: C, 35.76; H, 6.00; S, 10.61. Found: C, 35.96; H, 6.20; S, 10.58.

Acknowledgements

We thank Ms. Christel Bernd and Mr. Günter Riethmüller at the Max Planck Institute for Medical Research, Heidelberg, for the high-resolution MS spectra and the elemental analyses. We also thank the Institute for Organic Chemistry, University of Heidelberg, for use of their spectropolarimeter.

References

1. Torchilin, V. P. *Eur. J. Pharm. Sci.* **2000**, *11*(Suppl. 2), 81–91.
2. Dubowchik, G. M.; Walker, M. A. *Pharm. Ther.* **1999**, *83*, 67–123.
3. Flier, J. S.; Mueckler, M. M.; Usher, P.; Lodish, H. F. *Science* **1987**, *235*, 1492–1495.
4. Strauss, L. G.; Conti, P. S. *J. Nucl. Med.* **1991**, *32*, 623–648.
5. Hatanaka, M. *Biochim. Biophys. Acta* **1974**, *355*, 77–104.
6. Bagshawe, K. D. *Cell Biophys.* **1994**, *24-25*, 83–91.
7. Lostao, M. P.; Hirayama, B. A.; Loo, D. D.; Wright, E. M. *J. Membr. Biol.* **1994**, *142*, 161–170.
8. Díez-Sampedro, A.; Lostao, M. P.; Wright, E. M.; Hirayama, B. A. *J. Membr. Biol.* **2000**, *176*, 111–117.
9. Pohl, J.; Bertram, B.; Hilgard, P.; Nowrousian, M. R.; Stüben, J.; Wiessler, M. *Cancer Chemother. Pharmacol.* **1995**, *35*, 364–370.
10. Stüben, J.; Port, R.; Bertram, B.; Bollow, U.; Hull, W. E.; Schaper, M.; Pohl, J.; Wiessler, M. *Cancer Chemother. Pharmacol.* **1996**, *38*, 355–365.
11. Veyhl, M.; Wagner, K.; Volk, C.; Gorboulev, V.; Baumgarten, K.; Weber, W. M.; Schaper, M.; Bertram, B.; Wiessler, M.; Koepsell, H. *Proc. Natl. Acad. Sci. U.S.A.* **1998**, *95*, 2914–2919.
12. Briasoulis, E.; Judson, I.; Pavlidis, N.; Beale, P.; Wanders, J.; Groot, Y.; Vermaan, G.; Schuessler, M.; Niebch, G.; Siamopoulos, K.; Tzamakou, E.; Rammou, D.; Wolf, L.; Walker, R.; Hanauske, A. *J. Clin. Oncol.* **2000**, *18*, 3535–3544.
13. Webley, S. D.; Francis, R. J.; Pedley, R. B.; Sharma, S. K.; Begent, R. H.; Hartley, J. A.; Hochhauser, D. *Br. J. Cancer* **2001**, *84*, 1671–1676.
14. Syrigos, K. N.; Rowlinson-Busza, G.; Epenetos, A. A. *Int. J. Cancer* **1998**, *78*, 712–719.
15. Tietze, L. F.; Hannemann, R.; Buhr, W.; Logers, M.; Menningen, P.; Lieb, M.; Starck, D.; Grote, T.; Doring, A.; Schuberth, I. *Angew. Chem.* **1996**, *35*, 2674–2677.
16. Yarbro, J. W. *Sem. Oncol.* **1992**, *19*(Suppl. 9), 1–10.
17. Donehower, R. C. *Sem. Oncol.* **1992**, *19*(Suppl. 9), 11–19.
18. Walles, S.; Ehrenberg, L. *Acta Chim. Scand.* **1968**, *8*, 2727–2729.
19. Buggia, I.; Locatelli, F.; Regazzi, M. R.; Zecca, M. *Ann. Pharmacother.* **1994**, *28*, 1055–1062.
20. Schmidt, R. R. *Angew. Chem.* **1986**, *98*, 213–236.
21. Koenigs, W.; Knorr, E. *Ber. Dtsch. Chem. Ges.* **1901**, *34*, 957–960.
22. Lindhorst, T. K. *Essentials of Carbohydrate Chemistry and Biochemistry*; Wiley-VCH: Weinheim, 2000; pp 84–90.
23. Cao, S.; Tropper, F. D.; Roy, R. *Tetrahedron* **1995**, *51*, 6679–6686.

24. Helferich, B.; Werner, J. *Chem. Ber.* **1942**, *75B*, 1446–1452.
25. Zemplén, G.; Kunz, A. *Ber. Dtsch. Chem. Ges.* **1923**, *56*, 1705–1710.
26. Wong, T. C.; Rutar, V. *J. Am. Chem. Soc.* **1984**, *106*, 7380–7384.
27. Hull, W. E. In *Two-Dimensional NMR Spectroscopy: Applications for Chemists and Biochemists*, 2nd ed.; Croasmun, W. R., Carlson, R. M. K., Eds.; VCH: New York, 1994; pp 67–456.
28. Krishnamurthy, V. V.; Casida, J. E. *Magn. Reson. Chem.* **1987**, *25*, 837–842.
29. Praly, J. P.; Descotes, G. *Tetrahedron Lett.* **1982**, *23*, 849–852.
30. Petrig, J.; Schibli, R.; Dumas, C.; Alberto, R.; Schubiger, P. A. *Chem. Eur. J.* **2001**, *7*, 1868–1873.